Orientation of Simple Amides at the Bicelle−Water Interface of a Lyotropic Liquid Crystal

Christoph F. Weise and James C. Weisshaar*

Department of Chemistry, University of Wisconsin-Madison, 1101 University Avenue, Madison, Wisconsin 53706-1396

Received: January 30, 2003; In Final Form: April 23, 2003

Liquid crystal NMR (LX-NMR) spectra of seven different small amides (formamide, acetamide, *cis*- and *trans*-*N*-methylformamide, *trans*-*N*-methylacetamide, *N*,*N*-dimethylformamide, and *N*,*N*-dimethylacetamide) are obtained in the lyotropic liquid crystalline solvent cesium pentadecafluorooctanoate in water (CsPFO/water). Fits of the spectra to a model Hamiltonian yield magnetic dipolar couplings D_{ij} (where *i* and *j* label two nuclear spins). The D_{ij} are directly related to amide geometry and the details of the orientational distribution of the amide while it visits the bicelle−water interface. Using calculated gas-phase geometries, we extract the orientation tensor **S** for each amide to within a factor of ±1. As estimated by the rms magnitude of the eigenvalues of **S**, the amides vary by a factor of 30 in orientational strength in the following order: *trans*-*N*-methylacetamide ($S_{rms} = 0.0031$); formamide (0.0038); acetamide (0.010); *cis*-*N*-methylformamide (0.011); *trans*-*N*-methylformamide (0.066); *N*,*N*-dimethylformamide (0.105). *N*,*N*-dimethylacetamide orients very strongly, but the spectrum is too complex to analyze. The molecules *trans*-*N*-methylformamide and especially *N*,*N*-dimethylformamide orient sufficiently strongly to suggest that they must partition to the bicelle−water interface in preference over the bulk water by a factor of 2−3 or more in local concentration. Isomerization about the amide linkage increases orientation strength by a factor of 6 from *cis*-*N*-methylformamide to *trans*-*N*-methylformamide. The strength of orientation evidently depends primarily on the *position* of methyl groups. Strong orientation arises in all three molecules with *N*-methyl, rather than N−H, situated trans to the carbonyl group. Evidently, orientation strength depends only mildly on the total number of methyl groups or on the molecular shape; nor is the electric dipole moment a key factor. A methyl group trans to the carbonyl group allows the carbonyl group to access the hydrogen-bonding environment of the bicelle−water interface, while the methyl group simultaneously inserts in the fluorocarbon core of the CsPFO bicelle. Remarkably, the **S** tensors for the strong orienters are consistent with such a simple mechanism dominating the angular distribution of the amide within the bicelle−water interface.

I. Introduction

Liquid-crystal NMR (LX-NMR)[1] has proven to be a powerful tool for delineation of complex phase diagrams and determination of solution-phase structure for solutes ranging from small molecules to modest-sized proteins.[2−15] We recently used this method to study conformational preferences of alanine dipeptide in the water-based, lyotropic liquid crystalline medium cesium pentadecafluorooctanoate in water (CsPFO/H_2O). At sufficiently high concentration and sufficiently low temperature, CsPFO assembles into oblate, disk-shaped bicelles[8] that align locally to form a liquid crystalline phase.[16] In the magnetic field of an NMR spectrometer, the bicelles throughout the sample align their symmetry axes parallel to the field. Transient encounters between a water-soluble peptide or amide and the oriented disks transfer net orientation to the solute, giving rise to direct *magnetic dipolar couplings* that depend sensitively on solute geometry and orientational distribution in known fashion. The alanine dipeptide study[17] found that a single conformation known as polyproline-II (P_{II}) fit 13 dipolar couplings within experimental error using five parameters to define the orientational properties. However, there remains the possibility that a second conformer, most likely right-handed alpha helix (α_R), is present in aqueous solution but orients only very weakly in the CsPFO liquid crystal.

Here, we apply LX-NMR to study the entire family of mono-, di-, and trimethyl-substituted formamides to better understand how small peptides orient in CsPFO/water.[17] We find that the orientation strength increases a surprising factor of 30 from formamide to *N*,*N*-dimethylformamide (*N*,*N*-DMF). The couplings in *N*,*N*-DMF are so large as to require preferential partitioning to the interface. In addition, mere cis−trans isomerization about the peptide bond increases orientation strength by a factor of 6 from *cis*-*N*-methylformamide (*cis*-NMF) to *trans*-NMF. The latter orients comparably to *N*,*N*-DMF. The strength of orientation does not depend primarily on the number of methyl groups. Rather, a rule of thumb that applies across the entire family is that the presence of a methyl group trans to the carbonyl group correlates with strong orientation.

By assuming gas-phase geometries from electronic structure calculations for each amide, we derive the orientation tensor **S** to within a sign. Detailed study of formamide and *N*,*N*-dimethylformamide shows that **S** changes very little for more sophisticated treatments including use of equilibrium geometries more appropriate for amides in a hydrogen-bonding medium,[18] use of a Boltzmann-weighted treatment of methyl rotor internal rotation, and application of vibrational corrections to internuclear distances.[19,20] A simple estimate indicates that the "strong

* To whom correspondence should be addressed. E-mail: weisshaar@chem.wisc.edu.

10.1021/jp034258y CCC: $25.00
Published on Web 05/31/2003

orienters" *N*,*N*-DMF and *trans*-NMF preferentially partition to the interface by a factor of 2 or more in concentration and must also orient to a very large degree while visiting the interface. The orientation tensors of both the strong orienters and the "moderate orienters" *cis*-NMF and acetamide are qualitatively consistent with a strong preference to place the carbonyl group in the hydrogen-bonding bicelle−water interfacial environment while simultaneously inserting one or more methyl groups into the fluorocarbon core of the bicelles. Adaptation of this idea to alanine dipeptide can also explain its orientational preferences in CsPFO/water.[17,21,22]

Earlier work demonstrated the importance of conformational *shape* in orienting nonpolar, flexible hydrocarbon solutes in thermotropic liquid crystals.[4,23] Linear hydrocarbon conformations are more highly populated in these solvents (which consist of stiff, linear solvent molecules) than in isotropic solutions in small-molecule solvents. For small proteins dissolved in lyotropic, phospholipid-based liquid crystals, recent work shows quantitative agreement between the orientation tensors and simple models based on shape for uncharged lipids and on shape plus electric field interactions for charged proteins and lipids.[24] In contrast, for small amides in CsPFO/water, we rule out both molecular shape and the interaction of the interfacial electric field with the amide dipole moment as important factors in the orientation mechanism. Instead, hydrogen bonding of carbonyl and amino groups with interfacial water and hydrophobicity of methyl groups evidently provide the dominant orientational forces in CsPFO/water.

II. Experimental Techniques

At 42 wt % in water, cesium pentadecafluorooctanoate (CsPFO) forms a lyotropic liquid crystal comprising oblate, disk-shaped *bicelles* about 22 Å thick and 80 Å in diameter (aggregation number about 190) that occupy roughly 24% of the volume of the solution.[8] When heated to the isotropic phase (above 37 °C) and then cooled in the strong magnetic field of an NMR spectrometer, the bicelles form a *macroscopically oriented phase* with its director—the symmetry axis of the mean field—aligned parallel to the magnetic field. In LX-NMR, the liquid crystalline solvent medium subjects the solute to an *orientationally anisotropic mean field*.[2] The orientational mean field in CsPFO/D_2O is stronger than that in phospholipid-based systems recently used in studies of larger biological molecules.[11] Small water-soluble amides sample primarily an aqueous environment but acquire substantial orientation from transient encounters with the oriented bicelles, resulting in moderately strong intramolecular direct magnetic dipolar couplings between nuclear spins. Analysis of such LX-NMR spectra yields the dipolar couplings, D_{ij}. With an approximate geometry from theory as input, the set of dipolar couplings yields a best-fit tensor **S** describing the amide orientational distribution in space, the primary subject of this work.

CsPFO was prepared as follows. Equimolar amounts of cesium carbonate and pentadecafluorooctanoic acid were dissolved in 50:50 hexane/butanol through gentle heating to 40 °C and mild stirring. The product was recrystallized twice from 50:50 butanol/hexane and was dried in a vacuum oven at 60 °C to remove residual solvent, purity being verified by NMR. The amide solute, surfactant, and water were weighed into an NMR tube to make approximately 1 g of sample with a solute concentration of ∼50 mM. The samples were heated to the isotropic phase (∼40 °C) and mixed in the NMR tube to obtain a homogeneous solution. Proton spectra acquired at this higher temperature are liquidlike with fairly narrow lines (1.5 Hz fwhm) and the usual scalar couplings. In all cases, the temperature was regulated to ±0.1 °C. Typical mole fractions in our samples are 0.977 water, 0.020 CsPFO monomers, and 0.003 amide. The aqueous component was either D_2O (in which case all amino protons are exchanged to deuterium) or H_2O buffered at pH 5 (in which case the amino protons exchange slowly). In two cases, formamide and *N*,*N*-DMF, a ^{15}N label provides additional dipolar couplings and eliminates broadening of certain proton resonances arising from ^{14}N quadrupolar relaxation. In general, the transition temperature from nematic phase to isotropic phase in the CsPFO occurred at the same temperature reported by Boden et al.[16] to within roughly 1 °C, as judged by the sharp onset of dipolar couplings as the temperature was slowly lowered. For *N*,*N*-DMF, the reported spectrum was obtained at mole fraction of 0.0005. For *N*,*N*-DMF alone, the transition temperature decreased markedly with mole fraction above 0.0005, as described below.

Spectra of the various amides were obtained for samples having CsPFO in the range 34−42 wt %. Over this range, the isotropic/liquid crystal phase transition occurs at temperatures in the range 28−37 °C. LX-NMR spectra were obtained at 18−28 °C, always at least 8 °C below the transition temperature.[16] For a given weight percent of CsPFO, the strength of orientation increases rapidly as the temperature decreases over the first 5 °C below the phase transition and then levels off abruptly. Evidently, the bicelles reach maximum orientation over that temperature range. For temperatures more than 5 °C below the phase transition, the degree of orientational order for a given amide increases about 30% over the range 34−42 wt % CsPFO, as judged by *N*,*N*-DMF. The choice of CsPFO weight percent in this study was governed primarily by the search for conditions that make sharp, well-resolved dipolar coupled spectra amenable to analysis. The weakly orienting amides were studied at higher CsPFO weight percent to increase dipolar couplings, which yields a more accurate **S** matrix. The amides that orient most strongly were naturally studied at the lowest CsPFO weight percent, that is, under the *least orienting* conditions, to keep the spectra tractable. Therefore, the strong observed variation in degree of orientation among amides is *not* due to different weight percent CsPFO. If anything, our comparisons *underestimate* differences between weakly and strongly orienting amides by about 30%.

One-dimensional 500 MHz proton spectra were acquired with a pulse-observe sequence in the ^1H channel. The frequency lock was turned off. In some spectra, a GARP decoupling sequence[25] was used in the ^2H channel with the decoupler power selected as a compromise between optimal decoupling and minimal heating of the sample. For the spectra taken in H_2O, the water resonance in the ^1H spectra was saturated with a presaturation pulse. To acquire sufficient S/N, 2−64 transients were accumulated at a minor cost to resolution due to slight fluctuations in the magnetic field during the acquisition due to the absence of a spin lock. The number of points collected was 32 000−130 000 with sweep width of 8−13 kHz for a spectral resolution of 0.12−0.24 Hz.

For clarity, we have labeled analogous protons in the different substituted formamides similarly. In formamide, we label the formyl proton $^1H^{form}$, the amino proton cis to the carbonyl $^1H^{cis}$, and the amino proton trans to the carbonyl $^1H^{trans}$. The latter two protons are magnetically inequivalent due to slow cis−trans isomerization on the NMR time scale. When the formyl proton is substituted by methyl, we label the three equivalent protons $^1H^{ac}$ after the acetyl group. Protons within methyl substituents on nitrogen are simply labeled $^1H^{cis}$ and $^1H^{trans}$

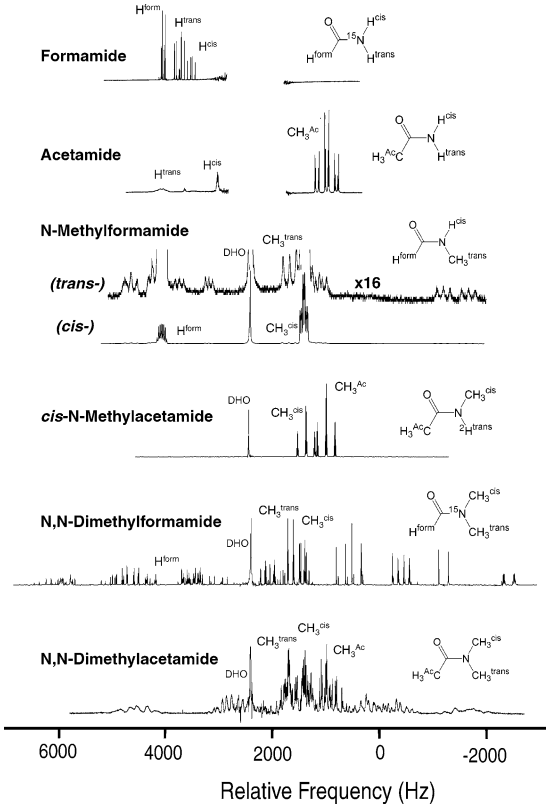

Figure 1. Proton NMR spectra at 500 MHz for various amides dissolved in CsPFO/water liquid crystalline medium. The weight percent of CsPFO and the temperature for each spectrum are given in the following figures. In the relative frequency scale 0 Hz corresponds to the chemical shift of tetramethylsilane (0 ppm in the usual scale). Correlation of specific proton types with spectral features is indicated.

according to the position of the methyl group relative to the carbonyl. Two of the compounds have ^{15}N labels. Samples in D_2O exchange spin-one deuterons ^{2}H for any amino protons present, which gives rise to weak ^{2}H$-^1$H dipolar couplings, which are sometimes resolved in the proton spectrum.

III. Results

A. Overview of Analysis. *1. Dipolar Coupling Constants from Oriented Spectra.* The Hamiltonian governing nuclear spin coupling in an anisotropic medium is well-known:

$$\hat{H} = -\sum_i (1-\sigma_i)\nu_0 \hat{I}_{zi} + \sum_{i<j}(J_{ij}+2D_{ij})\hat{I}_{zi}\hat{I}_{zj} + \frac{1}{2}\sum_{i<j}(J_{ij}-D_{ij})(\hat{I}_i^+\hat{I}_j^- + \hat{I}_i^-\hat{I}_j^+) \quad (1)$$

with i and j labeling different magnetic nuclei.[2,23] The scalar and dipolar coupling constants J_{ij} and D_{ij} appear beside the same spin operators. The first term is the effective chemical shift in the anisotropic medium. The dipolar and scalar coupling constants arise in different combinations in the second term (diagonal, first-order coupling) and the third term (off-diagonal, second-order coupling). In favorable circumstances, this allows unambiguous determination of the sign of D_{ij} when the sign of the corresponding J_{ij} is known by other means.

The oriented NMR spectra of formamide, acetamide, *cis*- and *trans*-*N*-methylformamide, *cis*-*N*-methylacetamide, and *N*,*N*-dimethylacetamide (*N*,*N*-DMF) are presented on the same relative frequency scale in Figure 1. Cursory examination of the spectra shows that the LX medium significantly orients all of the amides studied and that certain dipolar couplings are as large as 100−1000 Hz, much larger than scalar couplings. The molecules divide into three classes. The degree of orientation is weak for formamide and acetamide, moderate for *cis*-*N*-methylformamide and *N*-methylacetamide, comparable to that observed earlier for alanine dipeptide, and strong for *trans*-*N*-methylformamide, *N*,*N*-dimethylformamide, and *N*,*N*-dimethylacetamide. The weakly and moderately oriented spectra are essentially first-order, exhibiting simple multiplet structure dominated by the D_{ij}, which nevertheless remain small compared with chemical shift differences $\sigma_i - \sigma_j$. In the strongly oriented spectra, dipolar couplings far exceed chemical shift differences and the spectra are more complex. Typical line widths were 1−3 Hz fwhm in the isotropic spectra and 3−10 Hz in the oriented spectra.

Analysis of the spectra proceeds in stages. The isotropic spectra are readily assigned from the pattern of J couplings. In the liquid crystalline samples, all chemical shifts move downfield (toward higher frequency) because of the change in magnetic susceptibility of the bulk. In addition, the net orientation of the solute averages each chemical shift tensor differently in the LX-NMR spectrum than in the isotropic spectrum, accounting for the *differential* change in chemical shifts among different sets of equivalent protons. Dipolar couplings produce 1:2:1 intramethyl triplets that are typically widely split because of the small internuclear distance. The central methyl peaks usually lie in the same order as they did in the isotropic spectrum. In spectra taken in D_2O, deuterium decoupling can sometimes change a broad, featureless envelope into sharp lines by eliminating dipolar coupling to the deuterons. The weakly and moderately oriented samples give spectra readily assigned; the mildly irregular pattern of some of the finer splittings and intensities is indicative of deviations from first-order coupling. For the more strongly oriented spectrum of *N*,*N*-DMF, one of the methyl group patterns is fairly clear while the other is badly mixed. Assignment is then more difficult and relies heavily on trial and error comparing calculated and experimental spectra. For *N*,*N*-dimethylacetamide, there are three methyl groups and so many strong couplings that we have not succeeded in assigning the spectrum.

Detailed quantitative analysis is carried out using the program XSIM (UNIX) or SpinWorks (MS Windows version) available from Dr. Kirk Marat (U. Manitoba),[26] which simulates dipolar-coupled spectra from a set of parameters in the multispin Hamiltonian of eq 1. Input parameters include adjustable chemical shifts, scalar couplings J_{ij} transferred from the isotropic spectra, and adjustable dipolar coupling constants D_{ij}. Once a good qualitative fit is obtained by manual adjustment of all parameters, hundreds or even thousands of calculated NMR transitions in the simulated spectrum are assigned by the user to corresponding resolved features in the experimental spectrum. This is a many-to-one mapping. The program optimizes a designated set of adjustable parameters to minimize the sum of squared errors in calculated vs experimental line frequencies. Good fits match the frequencies of lines within a small fraction of the line width and the detailed intensity patterns very well. The small remaining systematic intensity deviations between experiment and the best-fit simulations occur because differential line-broadening mechanisms are neglected and also because XSIM improperly fits many lines of slightly different calculated frequency to the *center* frequency of each resolved feature. The accuracy of the magnitudes of the best-fit D_{ij} is judged semiquantitatively by systematically varying the value of each coupling while optimizing all remaining parameters. The stated

uncertainties in the tables take into account this fitting error and the spectral resolution.

The sign of each D_{ij} has physical meaning; for proton−proton couplings, negative values indicate preferential orientation of the internuclear vector along the *z*-axis (magnetic field direction) while positive values indicate preferential orientation near the *xy* plane. First-order spectra are insensitive to the pattern of signs chosen in the fitting procedure, in which case we can extract only the magnitudes $|D_{ij}|$. In the strongly coupled spectra, the frequencies and intensities of lines can be exquisitely sensitive to the pattern of signs of the D_{ij}. For formamide and for *N*,*N*-DMF, we obtained substantial relative sign information from the intensity patterns and some absolute sign information due to one or more large scalar couplings J_{ij}, of which the sign is known independently.

2. Fits to Geometries from Theory. The dipolar coupling between nuclei *i* and *j* depends on the internuclear distance r_{ij} and on the angular distribution of the vector $\mathbf{r}_{ij}$ in space:[23]

$$D_{ij} = -K_{ij}\langle r_{ij}^{-3} P_2(\cos\theta_{ij})\rangle \tag{2a}$$

$$\cong \frac{2}{3}\,\mathrm{Tr}(\mathbf{S}\mathbf{G}_{ij}) \tag{2b}$$

Here $K_{ij} = \mu_0\hbar\gamma_i\gamma_j/(8\pi^2)$, μ_0 being the nuclear magneton and γ_i the gyromagnetic ratio of nucleus *i*; θ_{ij} is the angle between $\mathbf{r}_{ij}$ and the *z*-axis (magnetic field axis), and P_2 is the second Legendre polynomial, $P_2(x) = (3x^2 - 1)/2$. The brackets indicate an average over all motion of the molecule, including internal rotation of methyl groups, molecular vibration, translation relative to the bicelle−water interface, and overall molecular reorientation in space. Equation 2a is quite general. Equation 2b assumes that vibrational and methyl torsional motions separate from tumbling in space, that is, that averaging of the internal geometry is fast on the time scale of reorientation.[2,4] The average in eq 2a then factors. **S** is the symmetric, traceless 3 × 3 orientation tensor describing the angular distribution in space of a set of molecule-fixed Cartesian axes. $\mathbf{G}_{ij}$ is the 3 × 3 "geometry matrix" for the *ij* coupling, consisting of r_{ij}^{-3} times products of projection cosines of the *ij* internuclear vector onto the same molecule-fixed axes. The amides of interest here have a plane of symmetry when the geometry is averaged over methyl internal rotation and out-of-plane vibrations so that **S** has only three independent elements.[27] For a single conformer the orientation of which is independent of internal geometry, we can also write

$$D_{ij} \cong -K_{ij}S_{ij}\langle r_{ij}^{-3}\rangle \tag{3}$$

where the orientational order parameter of $\mathbf{r}_{ij}$ is $S_{ij} = \langle P_2(\cos\theta_{ij})\rangle$. For intramethyl ^{1}H−^{1}H couplings, we report the order parameter for the methyl rotor symmetry axis and not that for the interproton vectors. This is obtained from the motionally averaged order parameter for the ^{1}H−^{1}H vectors on multiplication by −2.[6]

For formamide, we carried out a detailed investigation of the range of solution-phase geometries consistent with the dipolar couplings, including effects of internal vibrational motion.[22] For the methyl-substituted formamides, we use a simpler procedure that yields the orientational properties to good accuracy. For each molecule, we carried out electronic structure calculations to optimize the *gas-phase* geometry (Gaussian 98, B3LYP/6-31+G(d,p)).[28] Detailed coordinates are given in Supplementary Table S2 in Supporting Information. These equilibrium geometries serve as input to eq 2b, which is solved in a least-squares sense for the three independent **S** matrix elements that optimize the calculated D_{ij}. We accounted for the rapid torsion of the methyl groups by averaging the fitting parameters over such motions. For B3LYP calculations that optimize the entire geometry as a function of the internal rotation dihedral angle α, the methyl geometry varies subtly with α. In all cases, the methyl rotor geometry was assumed to be tetrahedral with CH = 1.10 Å, and HCH and HCC/N = 109.5°. The torsional angle distribution of the hydrogen atoms was described either as uniform or as a Boltzmann distribution within the calculated potential of the form $E = (U/2)(1 - \cos 3\alpha)$. The barrier height varies from 0.3 to 3.0 kcal/mol across all molecules in this study.[29] Only for *N*,*N*-DMF did the quality of fit depend sensitively on details of the methyl rotor treatment. Fortunately, the **S** matrix is remarkably insensitive to such details, as described quantitatively below.

It quickly becomes obvious that many of the sign combinations that fit the spectrum well (section 1) are not physically realizable for sensible amide geometries. For the acceptable sign combinations, best-fit rms errors for the calculated dipolar couplings are typically <1 Hz and comparable to the rms uncertainty in the couplings themselves. For the unacceptable sign combinations, best-fit rms errors are measured in tens of hertz or more. In most cases, the combination of spectral fitting with XSIM and fitting of dipolar couplings using the gas-phase geometry in eq 2b eliminates all but two sign combinations. Moreover, those two combinations are typically related to each other by a change in sign of the first-order parameter ($J_{ij} + 2D_{ij}$) *for all pairs of spins simultaneously*. This amounts to simultaneous inversion of the signs of all of the dipolar couplings, because $2D_{ij}$ is typically much larger than J_{ij}.

Thus we usually obtain complete *relative* sign information for the D_{ij} and a meaningful best-fit orientation tensor **S**, also to within a sign. The best-fit orientation tensor **S** is diagonalized to obtain the three principal values (eigenvalues) S_a, S_b, and S_c and the orientation of the principal axes relative to the molecular frame. Because two axes must lie in the molecular plane and one perpendicular to the plane, the orientation of the principal axes is determined by a single in-plane angle. Using the gas-phase geometry in eq 3, we obtain a set of orientational order parameters S_{ij}, also with known relative signs. For intramethyl couplings, these refer to the orientation of the methyl rotor symmetry axis. Our focus will be on the tensor **S** and the order parameters S_{ij}.

The fits of dipolar couplings to the gas-phase geometries without corrections for vibrational effects are quantitatively good. When only four relative D_{ij} are extracted from the spectrum, the rms error between calculated and observed coupling always lies within the experimental error. The more rigorous formamide study shows that this is probably fortuitous, that is, subtle adjustments in the **S** matrix compensate for the incorrect equilibrium geometry and for the absence of vibrational corrections. Fortunately, the same formamide study indicates that the orientation parameters of interest here are quite insensitive to details of geometry and treatment of internal motion, ensuring that the present results are physically meaningful.

B. Formamide. We analyzed isotropic and oriented ^{1}H spectra of ^{15}N-labeled formamide in 42 wt % CsPFO at 40 and 22 °C, respectively. Use of ^{15}N-labeled formamide increased the number of measurable couplings and also eliminated broadening caused by rapid relaxation of the quadrupolar ^{14}N nucleus. The sample was prepared at pH = 5.0 to minimize the hydrogen-exchange rate. A fit to the isotropic spectrum revealed the magnitudes of the *J*-couplings shown in Table 1. The signs

TABLE 1: Best-fit Parameters from Dipolar-Coupled NMR Spectrum of ^{15}N-Formamide in 41.7 wt % CsPFO/H_2O at 22.0 °C

	expt		calcd from gas-phase geometry		
vector[a]	J_{ij} (Hz)[b]	D_{ij} (Hz)[c]	D_{ij} (Hz)	r_{ij} (Å)[d]	S_{ij}[e]
$^{15}N-H^{form}$	−13.8	−5.5 ± 0.4	−5.1	2.06	−0.0040
$^{15}N-H^{trans}$	−91.4	+30.1 ± 0.4	+30.5	1.01	+0.0025
$^{15}N-H^{cis}$	−88.7	−59.1 ± 0.4	−59.5	1.01	−0.0050
$^{1}H^{form}-^{1}H^{trans}$	+2.1	−1.3 ± 0.4	−1.1	2.32	+0.00014
$^{1}H^{form}-^{1}H^{cis}$	+13.8	+23.1 ± 0.4	+21.3	2.97	−0.0051
$^{1}H^{cis}-^{1}H^{trans}$	+2.0	+42.4 ± 0.4	+42.5	1.74	−0.0019

[a] See Figure 8. [b] From isotropic spectrum at 40 °C. [c] From XSIM fits to dipolar-coupled spectrum. Signs are completely determined.[d] Gas-phase internuclear distance. Details in Supplementary Table S2 (Supporting Information). [e] Order parameters calculated from eq 3 and gas-phase r_{ij}.

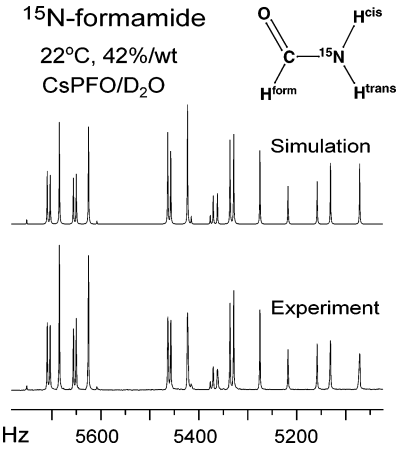

Figure 2. LX-NMR spectrum (lower trace) of ^{15}N-labeled formamide in 42 wt % CsPFO/D_2O at pH = 5.0 and 22.0 °C and XSIM spectral simulation (upper trace) using parameters in Table 1. Simulation line width is 1.4 Hz fwhm.

of the *J*-couplings are taken from the literature.[30] Our values for the couplings to nitrogen, which are particularly sensitive to the solvent conditions, differ by less than 0.3 Hz from the values in dilute aqueous solutions reported in the literature.[19,31] H^{cis} and H^{trans} give rise to separate resonances due to slow torsional exchange about the amide bond. We assigned these protons on the basis of the couplings to H^{form}. The H^{trans} resonance in the isotropic spectrum is ∼350 Hz upfield from the formyl resonance and ∼150 Hz downfield from the H^{cis} resonance.

The oriented spectrum and its best-fit simulation are presented in Figure 2. Formamide orients very weakly on the scale of the other amides studied. Nevertheless, the spectrum is not a simple superposition of first-order patterns due to the close proximity of the three proton chemical shifts. Analysis of the dipolar coupled spectrum of ^{15}N-labeled formamide yields six dipolar couplings as given in Table 1. Our ability to fit the experimental spectrum was unaffected by changes of ∼5 Hz in the simulation values of the larger *J*-couplings because these changes could be compensated for by adjusting the dipolar couplings. We therefore held the *J*-couplings constant at the values from the isotropic spectrum. The signs of all of the scalar couplings are known, and in this case, their magnitude is often comparable to the corresponding dipolar couplings. This leads to an ambiguity in both sign and magnitude for the D_{ij} because of the two ways to obtain the same $|J_{ij} + 2D_{ij}|$. However, only one sign combination is consistent with sensible formamide geometries, and these are given in Table 1. In this case alone,

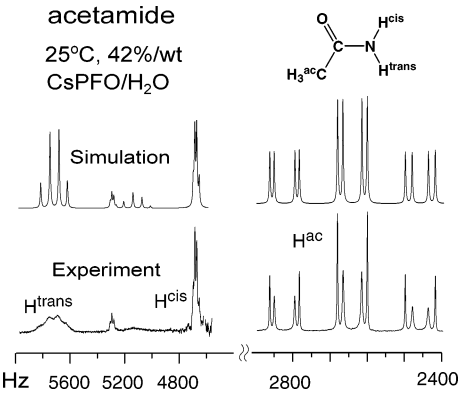

Figure 3. LX-NMR spectrum (lower trace) of acetamide in 41.6 wt % CsPFO/H_2O at pH 5.0 and 25.0 °C. The FID signal was multiplied by a 0.3 Hz Lorentzian apodization function to suppress noise. The upper trace shows the XSIM spectral simulation using parameters in Table 2. Simulation line width is 3.0 Hz fwhm in methyl region and 9.0 Hz fwhm in amino region.

the combination of spectral fitting and geometry determines all signs of D_{ij} and S_{ij}, as well as the signs of the elements of **S** and its eigenvalues. Fitting of the dipolar couplings to the calculated gas-phase geometry is fairly successful, producing rms error of 0.8 Hz compared with rms uncertainty of the couplings themselves of 0.4 Hz.

C. Acetamide. The dipolar-coupled spectrum (Figure 3) shows stronger orientation than formamide. The region of the two inequivalent amino protons is complicated by second-order dipolar coupling effects, as well as strong differential line broadening in all regions. In Figure 3, we fit the methyl region with a single line width of 3.0 Hz fwhm. Careful inspection shows that the seemingly attenuated lines are about twice as wide as their nearest neighbors, so the integrated intensities of the experimental methyl lines are actually in agreement with the simulation. We fit the $-NH_2$ region with a different single line width of 9.0 Hz, which matches half of the region well but is far too narrow for the other half, of which the line width is about 60 Hz fwhm. The cause of these different line widths is presumably the different coupling strength (both scalar and dipolar) to the ^{14}N nucleus, which itself undergoes quadrupolar relaxation. Again, the integrated intensities match well between experiment and simulation.

We extract four dipolar coupling magnitudes from the spectrum, yielding 16 possible sign combinations. Attempts to fit the 16 combinations to the gas-phase geometry show that only the two combinations listed in Table 2 are physically realizable. These are related by simultaneous inversion of all signs, that is, the geometry fits point to a unique set of *relative* signs. This in turn allows us to extract a physically meaningful **S** matrix to within a sign and the corresponding order parameters S_{ij} with relative signs determined (Table 2). The gas-phase geometry fits the dipolar couplings very well, having rms error of 0.2 Hz.

D. *cis*-*N*-Methylformamide and *trans*-*N*-Methylformamide (NMF). The oriented ^{1}H NMR spectrum of *N*-methylformamide in 35.5 wt % CsPFO at 20.0 °C and neutral pH is shown in Figure 4. Solvent exchange resulted in complete deuteration of the amido hydrogen atom. The exchange rate with solvent is sufficiently slow to allow us to extract $^{1}H-^{2}H$ dipolar couplings. Due to slow isomerization about the amide bond, separate resonances are observed for the isomers having the methyl group in cis and trans position relative to the carbonyl group. The cis species represents ∼90% of the total NMF population.[32] The simulation of the spectrum uses values of the *J* couplings

TABLE 2: Best-Fit Parameters from Dipolar-Coupled NMR Spectrum of Acetamide in 41.6 wt % CsPFO/H_2O at 25.0 °C

	expt		calcd from gas-phase geometry		
vector[a]	J_{ij} (Hz)[b]	D_{ij} (Hz)[c]	D_{ij} (Hz)	r_{ij} (Å)[d]	S_{ij}[e]
$^1H^{ac}-^1H^{ac}$		+60.9, −60.9 (±0.4)	+61.0	1.80	+0.0059, −0.0059
$^1H^{ac}-^1H^{cis}$	+0.4	+1.6, −2.0 (±0.4)	+2.0	3.82	−0.00074, +0.00093
$^1H^{ac}-^1H^{trans}$	+0.6	+37.9, −38.5 (±0.4)	+37.8	2.83	−0.0071, +0.0072
$^1H^{cis}-^1H^{trans}$	+2.0	−305.5, +303.5 (±0.4)	−305.5	1.74	+0.0135, −0.0134

[a] See Figure 8. [b] From isotropic spectrum at 40 °C. [c] From XSIM fits to dipolar-coupled spectrum. Entries refer to values in the two solution sets consistent with the spectrum and molecular geometry (estimated uncertainty in parentheses). [d] Gas-phase internuclear distance, averaged over methyl torsion. Details in Supplementary Table S2 (Supporting Information). [e] Order parameters calculated from eq 3 and gas-phase r_{ij}.

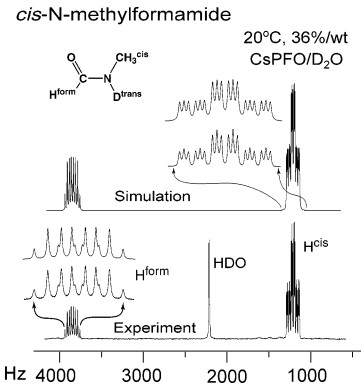

Figure 4. LX-NMR spectrum (lower trace) of *cis*-*N*-methylformamide in 35.5 wt % CsPFO/D_2O at 20.0 °C. Asterisks mark very weak lines from minority *trans*-NMF. The upper trace shows the XSIM spectral simulation using parameters in Table 3. Simulation line width is 5.5 Hz fwhm.

TABLE 3: Best-Fit Parameters from Dipolar-Coupled NMR Spectrum of *cis*-*N*-Methylformamide in 35.5 wt % CsPFO/D_2O at 20.0 °C

	expt		calcd from gas-phase geometry		
vector[a]	J_{ij} (Hz)[b]	D_{ij} (Hz)[c]	D_{ij} (Hz)	r_{ij} (Å)[d]	S_{ij}[e]
$^1H^{form}-^2H^{trans}$	+0.3	−24.1, +23.8 (±0.3)	−24.1	2.27	+0.0152, −0.0150
$^1H^{form}-^1H^{cis}$	−0.9	−13.2, +14.1 (±0.3)	−13.4	3.88	+0.0064, −0.0068
$^2H^{trans}-^1H^{cis}$	+0.8	+3.5, −4.3 (±0.3)	+3.2	2.64	−0.0035, +0.0042
$^1H^{cis}-^1H^{cis}$		+18.7, −18.7 (±0.3)	+18.6	1.80	+0.00180, −0.00180

[a] See Figure 8. [b] From isotropic spectrum at 40 °C. [c] From XSIM fits to dipolar-coupled spectrum. Entries refer to values in the two solution sets consistent with the spectrum and molecular geometry (estimated uncertainties in parentheses). [d] Gas-phase internuclear distance, averaged over methyl torsion. Details in Supplementary Table S2 (Supporting Information). [e] Order parameters calculated from eq 3 and gas-phase r_{ij}.

obtained in neat NMF solution (Table 3). Because of the small size of the *J* couplings, this introduces negligible uncertainty into the dipolar couplings (<0.2 Hz). The homogeneous line width is 4 Hz for *cis*-NMF.

For the majority *cis*-NMF isomer (Figure 4), we can extract four dipolar couplings. The orientation strength is modest, all couplings being <25 Hz. The quality of the spectral fits is insensitive to sign changes among the dipolar couplings, so 16 coupling sets produced satisfactory fits to the spectrum. Thus the magnitudes but not the signs of the couplings could be determined. Once again, only the two sign combinations of the dipolar couplings in Table 3 can be sensibly fit using the calculated gas-phase geometry, and these are related by simultaneous inversion of all signs. Thus, we determine the relative signs of all of the D_{ij}, a meaningful **S** matrix within multiplication by −1, and relative order parameters S_{ij}, all given in Table 3. The gas-phase geometry is able to fit the four couplings with rms error of only 0.2 Hz, the same as the estimated uncertainty of the D_{ij}.

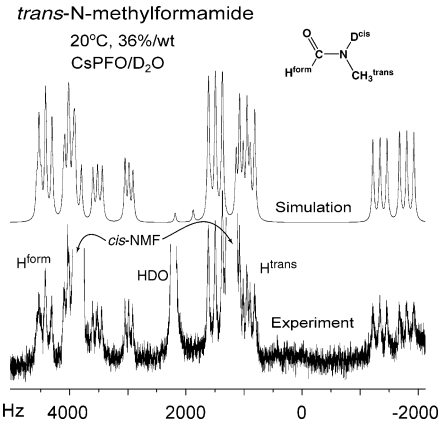

Figure 5. LX-NMR spectrum (lower trace) of *trans*-*N*-methylformamide in 35.5 wt % CsPFO/D_2O at 20.0 °C. A 1 Hz Lorentzian apodization function was applied to suppress noise. This is a more sensitive view of the spectrum in Figure 3. The upper trace shows the XSIM spectral simulation using parameters in Table 4. Simulation line width is 35 Hz fwhm.

The oriented spectrum of the minority *trans*-NMF is shown in Figure 5; a few of the same features are just discernible above the baseline in Figure 4. In complete contrast to the simple spectrum of *cis*-NMF, the trans isomer exhibits resonances dispersed over some 6000 Hz. The *trans*-NMF spectrum has 20 times smaller S/N due to its smaller population, the 30 Hz line width, and the plethora of lines. The simulated spectrum was optimized by trial and error and not by the automated fitting routine in XSIM. Once we found a set of dipolar couplings with XSIM that fit the *trans*-NMF spectrum well, we derived 15 more sets of couplings by permuting signs and attempted to fit the spectrum with the new sets by trial and error. Only four sign combinations fit the spectrum well. The four successful fits have opposite signs for $D(^2H^{cis}-^1H^{trans})$ and $D(^2H^{cis}-^1H^{form})$ and opposite signs for $D(^1H^{trans}-^1H^{form})$ and $D(^1H^{trans}-^1H^{trans})$. The uncertainty in the dipolar couplings is 2−3 Hz compared with magnitudes of 40−950 Hz.

Of the four coupling sets that reproduced the experimental spectrum, only the two included in Table 4 could be fit reasonably well using the calculated gas-phase structure of *trans*-NMF in eq 2. Once again, these two solutions are related by simultaneous inversion of the signs of all $(2D_{ij} + J_{ij})$. The fit of four dipolar couplings to the gas-phase geometry yields rms error of 0.8 Hz, small compared with the estimated rms uncertainty of 2.5 Hz. The derived parameters are collected in Table 4.

E. *trans*-*N*-Methylacetamide (*trans*-NMA). We call this molecule *trans*-*N*-methylacetamide in accord with organic nomenclature (*N*-methyl trans to acetyl methyl), but continue our convention of labeling the *N*-methyl protons as $^1H^{cis}$ because the methyl group lies cis to the carbonyl group. The oriented spectrum in 41.8 wt % CsPFO/H_2O at 28.0 °C and its simulation are shown in Figure 6. We saw no evidence of the *cis*-NMA

TABLE 4: Best-Fit Parameters from Dipolar-Coupled NMR Spectrum of *trans*-*N*-Methylformamide in 35.5 wt % CsPFO/D_2O at 20.0 °C

	expt		calcd from gas-phase geometry		
vector[a]	J_{ij} (Hz)[b]	D_{ij} (Hz)[c]	D_{ij} (Hz)	r_{ij} (Å)[d]	S_{ij}[e]
$^1H^{form}-^2H^{cis}$	+2.0	+39, −41 (± 2)	+38.8	2.95	−0.054, +0.057
$^1H^{form}-^1H^{trans}$	0.8	−243, +242 (±3)	−243	2.84	+0.046, −0.046
$^2H^{cis}-^1H^{trans}$	−0.5	−61, +61 (±3)	−59	2.62	+0.059, −0.060
$^1H^{trans}-^1H^{trans}$		+947, −947 (±2)	+947	1.80	+0.091, −0.091

[a] See Figure 8. [b] From isotropic spectrum at 40 °C. [c] From XSIM fits to dipolar-coupled spectrum. Entries refer to values in the two solution sets consistent with the spectrum and molecular geometry (estimated uncertainties in parentheses). [d] Gas-phase internuclear distance, averaged over methyl torsion. Details in Supplementary Table S2 (Supporting Information). [e] Order parameters calculated from eq 3 and gas-phase r_{ij}.

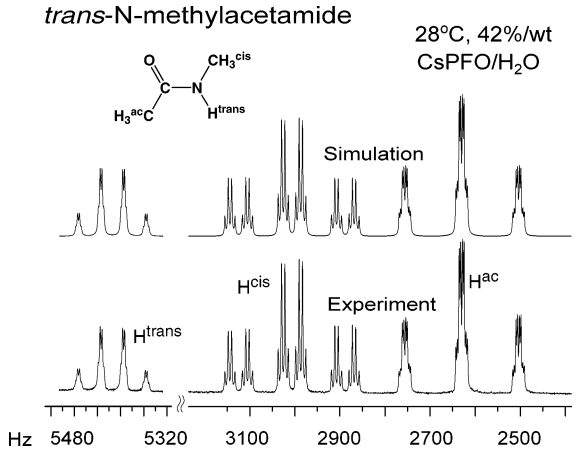

Figure 6. LX-NMR spectrum (lower trace) of *trans*-*N*-methylacetamide in 41.8 wt % CsPFO/H_2O at pH 5.0 and 28.0 °C and XSIM spectral simulation (upper trace) using parameters in Table 5. Simulation line width is 2.0 Hz fwhm.

isomer, consistent with the literature. The amino methyl protons are assumed to lie further downfield than the acetyl methyl protons on the basis of the usual assignment in isotropic spectra. The methyl group chemical shifts differ by 376 Hz compared with 373 Hz in the isotropic spectrum. Because the order parameters are small, changes in chemical shift *differences* on orientation should also be small (<50 Hz). The fits of the dipolar couplings to the gas-phase geometry are successful only with this assignment.

The magnitudes of the five proton−proton dipolar couplings are readily determined with XSIM (Figure 6), but the signs are ambiguous. As usual, the fitting of dipolar couplings to the gas-phase geometry narrows the possibilities to a pair of sign combinations related by simultaneous inversion of all signs. The rms fitting error is 0.3 Hz, comparable to the estimate of 0.4 Hz rms for the accuracy of the couplings themselves. The derived parameters are given in Table 5. *trans*-NMA is the one case for which the two possible choices of signs lead to corresponding eigenvalues of the **S** matrix of which the magnitudes differ substantially, as described in detail below.

F. *N*,*N*-Dimethylformamide (N,N-DMF). Our study of *N*,*N*-dimethylformamide was more extensive, including spectra of the unlabeled and the ^{15}N-labeled compound and also a systematic study of effects of solute concentration on the isotropic−nematic transition temperature and on chemical shift changes. The oriented ^1H spectrum of unlabeled *N*,*N*-DMF in 35 wt % CsPFO/D_2O at 21 °C is shown in Supplementary Figure S1 in Supporting Information. The spectrum is strongly coupled, exhibiting lines over a 5000 Hz frequency range, reminiscent of *trans*-NMF. The mean homogeneous line width is ∼10 Hz fwhm.

The $^1H-^1H$ *J*-couplings used in the simulations were obtained from the isotropic spectrum of ^{15}N-labeled *N*,*N*-DMF oriented in 34 wt % CsPFO/D_2O at 40 °C. They are small (<1 Hz) and were assumed positive (Table 6). Five proton−proton dipolar couplings are obtained from the unlabeled compound, and all 32 potential sign combinations were explored. Most of these could be quickly discarded because of the sensitivity of the strongly second-order spectral intensity patterns to the relative signs of different dipolar couplings. Four sign combinations (two

TABLE 5: Best-Fit Parameters from Dipolar-Coupled NMR Spectrum of *trans*-*N*-Methylacetamide in 41.8 wt % CsPFO/H_2O at 28.0 °C

	expt		calcd from gas-phase geometry		
vector[a]	J_{ij} (Hz)[b]	D_{ij} (Hz)[c]	D_{ij} (Hz)	r_{ij} (Å)[d]	S_{ij}[e]
$^1H^{ac}-^1H^{ac}$		−42.0, +42.0 (±0.4)	−40.4	1.80	−0.0041, +0.0041
$^1H^{cis}-^1H^{cis}$		−39.4, +39.4 (±0.4)	−40.5	1.80	−0.0038, +0.0038
$^1H^{ac}-^1H^{trans}$	−0.5	+1.8, −1.3 (±0.4)	+1.7	2.74	−0.00031, +0.00022
$^1H^{ac}-^1H^{cis}$	+0.3	+3.6, −3.9 (±0.4)	+3.4	4.71	−0.0031, +0.0034
$^1H^{cis}-^1H^{trans}$	+4.7	+17.1, −21.8 (±0.4)	+18.3	2.63	−0.0026, +0.0033

[a] See Figure 8. [b] From isotropic spectrum at 40 °C. [c] From XSIM fits to dipolar-coupled spectrum. Entries refer to values in the two solution sets consistent with the spectrum and molecular geometry (estimated uncertainties in parentheses). [d] Gas-phase internuclear distance, averaged over methyl torsion. Details in Supplementary Table S2 (Supporting Information). [e] Order parameters calculated from eq 3 and gas-phase r_{ij}.

TABLE 6: Best-Fit Parameters from Dipolar-Coupled NMR Spectrum of ^{15}N,^{15}N-Dimethylformamide in 34.0 wt % CsPFO/D_2O at 18.0 °C

	expt		calcd from gas-phase geometry		
vector[a]	J_{ij} (Hz)[b]	D_{ij} (Hz)[c]	D_{ij} (Hz)	r_{ij} (Å)[d]	S_{ij}[e]
$^{15}N-H^{form}$	−13.3	−41.2, +54.5 (± 0.5)	−30.6	2.06	−0.0294, +0.0390
$^{15}N-H^{trans}$	−1.4	+90.3, −88.9 (± 0.5)	+89.5	2.10	+0.0684, −0.0673
$^{15}N-H^{cis}$	−1.2	−50.4, +51.6 (± 0.5)	−52.6	2.10	−0.0382, +0.0391
$^1H^{form}-^1H^{trans}$	+0.7	−706.5, +705.8 (± 0.5)	−703.2	2.70	+0.116, −0.116
$^1H^{form-1}H^{cis}$	+0.6	+112.1, −112.7 (± 0.5)	+108.7	3.86	−0.0536, +0.0539
$^1H^{cis-1}H^{trans}$	0.0	−0.8, +0.8 (± 0.5)	−1.3	3.23	+0.0002, −0.0002
$^1H^{cis-1}H^{cis}$		−650.5, +650.5 (± 0.5)	−652.0	1.80	−0.0628, +0.0628
$^1H^{trans-1}H^{trans}$		+1108.2, −1108.2 (± 0.5)	+1100.0	1.80	+0.107, −0.107

[a] See Figure 8. [b] From isotropic spectrum at 40 °C. [c] From XSIM fits to dipolar-coupled spectrum. Entries refer to values in the two solution sets consistent with the spectrum and molecular geometry (estimated uncertainties in parentheses). [d] Gas-phase internuclear distance, averaged over methyl torsion. Details in Supplementary Table S2 (Supporting Information). [e] Order parameters calculated from eq 3 and gas-phase r_{ij}.

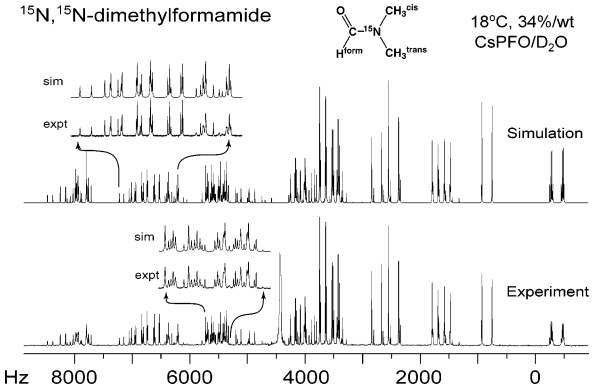

Figure 7. LX-NMR spectrum (lower trace) of $^{15}N,^{15}N$-dimethylformamide in 34.0 wt % CsPFO/D_2O at 18.0 °C. A 0.3 Hz Lorentzian apodization function was applied to suppress noise. The upper trace shows the XSIM spectral simulation using parameters in Table 6. Simulation line width is 3.0 Hz fwhm throughout.

pairs with partners related by simultaneous inversion of all signs) reproduce the spectrum well. One of these sets of couplings is provided as Supplementary Table S1 in Supporting Information. Although the successful simulation of the spectrum did not require an assignment of the methyl chemical shifts to particular groups in DMF, the subsequent structure fits did. We have assigned the upfield chemical shift in the oriented spectrum to the trans methyl group. This is the opposite of the assignment in water[33] and is based on the observed narrowing of the chemical shift difference between the cis and trans groups as the temperature increases in the oriented phase. The accuracy of the assignment of the downfield methyl resonances to the cis group was easily verified during fits of the dipolar couplings to reasonable DMF geometries.

The ^1H spectrum of ^{15}N-labeled *N*,*N*-DMF oriented in 34 wt % CsPFO/D_2O at 18 °C (Figure 7) helps resolve the sign uncertainty in the dipolar couplings. During spectral simulations the $^1H-^1H$ *J*-couplings were set to the values used in the fits for unlabeled DMF, while the $^1H-^{15}N$ *J*-couplings were obtained from an isotropic spectrum at 40 °C (spectrum not shown, couplings in Table 6). The sign of the *J*-coupling between ^{15}N and the formyl proton is negative,[6] which fixes the signs of the remaining $^1H-^{15}N$ *J*-couplings as positive according to Bourn and Randall.[33] In an attempt to test this sign assignment, we investigated the possibility that the $^{15}N-^1H_{methyl}$ *J*-couplings are either positive or negative, but accurate simulation of the oriented spectrum is possible in both instances.

The spectrum is so strongly coupled that it eliminates all but two sign combinations (Table 6). As usual these are related by simultaneous inversion of all signs. The fit of the eight dipolar couplings to the calculated gas-phase geometry is unusually poor, having rms error of 4.4 Hz compared with estimated uncertainty of 0.4 Hz rms. The poor fit of eight couplings to the gas-phase geometry and three independent **S** matrix elements contrasts sharply with the numerous good fits of only four couplings to three parameters for the other amides. This is due in part to the large magnitude of the couplings. In addition, DMF illustrates how eight highly accurate couplings more tightly constrain bond lengths and angles. The error is concentrated in three couplings, two of which involve the formyl proton. With very large dipolar couplings and two methyl rotors in close proximity, the fit of *N*,*N*-DMF couplings is unusually sensitive to details of geometry, methyl rotor treatment, and vibrational corrections. Fortunately, the **S** matrix is insensitive to these details, changing its principal values by less than 2%

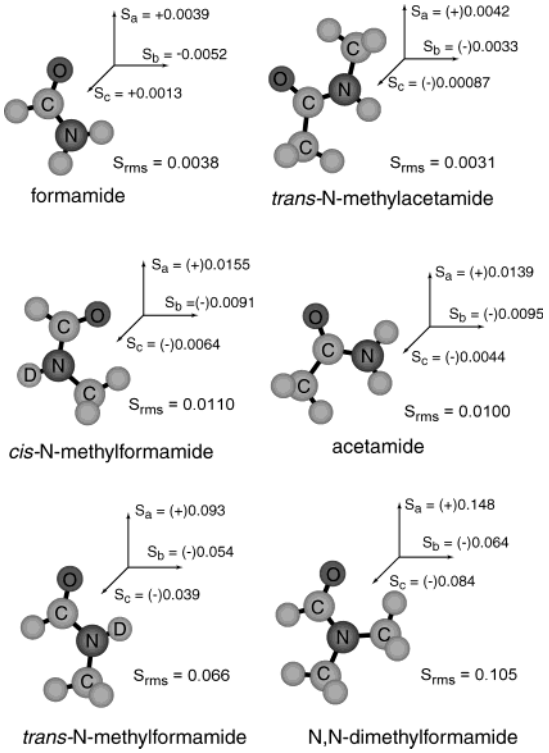

Figure 8. Orientation of amides relative to the molecule-fixed coordinate system in which the **S** matrix is diagonal. **S** matrices were obtained from fits to calculated gas-phase geometries of Supplementary Table S2 (Supporting Information). Eigenvalues along *a*-, *b*-, and *c*-axes and root-mean-square of eigenvalues are as shown. Absolute sign information is available for formamide only. In all other molecules, parentheses indicate that all three signs could be simultaneously inverted to obtain an **S** matrix consistent with the gas-phase geometry. S_{rms} is the root-mean-square of the eigenvalues.

and the orientation of its principal axes within the molecule by less than 3° over the entire range of sensible treatments.

G. Orientation of Amides at Bicelle−Water Interface. Using the calculated gas-phase geometry for each amide in eq 2b, we obtain a best-fit orientation tensor **S**, its three eigenvalues, and the orientation of the three principal axes relative to the molecular frame. Because both the unknown **S** matrix elements and the dipolar couplings appear linearly in eq 2b, the accuracy of the **S** matrix is directly related to the accuracy of the dipolar couplings themselves (Tables 1−6). For each amide, the largest dipolar couplings are typically accurate to 0.5−3%, and this is a good estimate of the fitting uncertainty in **S** for a given input geometry. In addition, the **S** matrix is remarkably insensitive to details of the input geometry, differences in treatment of methyl rotation, and inclusion or neglect of vibrational corrections. In the two cases most carefully studied, formamide and *N*,*N*-DMF, the three eigenvalues varied by less than 2% and the in-plane orientation of the molecule in the frame that diagonalizes **S** rotated by less than 3° over the entire range of treatments. This justifies an attempt to interpret rather subtle changes in the **S** matrix from molecule to molecule. Of course individual S_{ij} may vary by a wider percentage across geometric treatments when the relevant axis lies near the magic angle.

In Figure 8, we show the six amides placed in the molecule-fixed coordinate system that diagonalizes **S**, along with the eigenvalues S_a, S_b, and S_c. We consistently label the out-of-plane axis *c*, and the choice of *a*-axis is motivated by physical arguments below. The analysis yields absolute signs of the eigenvalues for formamide only. For all the other amides, we obtain only relative signs of the eigenvalues, as indicated by

the parentheses in Figure 8. Simultaneous inversion of all three signs is not ruled out. That is, any of the molecules except formamide can be rotated by 90° about the *c*-axis while the signs of all three eigenvalues are changed to yield an **S** matrix equally consistent with the experimental spectrum and geometric analysis. Except for *trans*-*N*-methylacetamide, the magnitudes of the three best-fit principal values vary less than 5% for the two different choices of sign. The sign choice in the figure associates a large, positive eigenvalue with the *a*-axis, as if it orients predominantly along the *z*-axis in space. The same sign choice always associates a large, negative eigenvalue with the other in-plane axis, the *b*-axis. Except for *N*,*N*-DMF, the out-of-plane eigenvalue S_c is then always the smallest in magnitude. S_c is then always negative, except for *trans*-NMA, for which it is very small. We discuss a plausible physical rationale for the upper sign choices being the correct ones below.

One measure of the strength of orientation of each molecule is the root-mean-square of the three eigenvalues of its **S** matrix. This measure divides seven amides into three groups. The "weak orienters" are formamide ($S_{rms} = 0.0038$) and *trans*-*N*-methylacetamide ($S_{rms} = 0.0031$). The "moderate orienters" are *cis*-*N*-methylformamide ($S_{rms} = 0.011$) and acetamide ($S_{rms} = 0.010$). The "strong orienters" are *trans*-*N*-methylformamide ($S_{rms} = 0.066$), *N*,*N*-dimethylformamide ($S_{rms} = 0.099$), and *N*,*N*-dimethylacetamide (spectrum not assigned, but strong dipolar coupling comparable to *N*,*N*-DMF). By this measure, the range of orientation strengths is a remarkable factor of 30. Simple cis−trans isomerization of *N*-methylformamide changes the orientation strength by a factor of 6.

Orientational order parameters $S_{ij} = \langle P_2(\cos \theta_{ij})\rangle$ for internuclear pairs were computed from eq 3 using values of r_{ij} from the calculated gas-phase geometries. The input geometries are given in detail in Supplementary Table S2 in Supporting Information. The principal axis system, in which **S** is diagonal (Figure 8), provides a convenient geometric interpretation of the orientational order parameter for any axis attached to the molecule. In that system, S_{ij} is simply the sum of the products of the projection cosine times the eigenvalue for each principal axis. Thus each eigenvalue is the orientational order parameter of the corresponding principal axis, and no molecule-fixed axis can have an order parameter that is more positive than the most positive eigenvalue or more negative than the most negative eigenvalue. S_{ij} equals +1 in the limit of perfect orientation along the *z*-axis, $-1/2$ in the limit of perfect orientation in the *xy* plane, and 0 in the limit of perfect orientation on the magic angle cone $\theta = 54.7°$. In all cases except formamide itself, we have only relative sign information about the S_{ij}. The upper signs in Tables 1−6 are chosen to be consistent with the upper sign choice for the eigenvalues in Figure 8. For the intramethyl couplings, S_{ij} in Tables 1−6 is the order parameter of the methyl rotor symmetry axis and not that of the interproton vectors themselves (section 2). For couplings among methyl-group protons or between methyl protons and other protons, the S_{ij} were derived by averaging geometries over an isotropic distribution of methyl rotor orientations.

IV. Discussion

A. Orientation Strength. Physical interpretation of the **S** matrix, its eigenvalues, and its molecule-fixed principal axes is inherently difficult. Because very different orientational distributions at the interface can be consistent with a given result, detailed motional models can be tested for consistency with the **S** matrix but never proven. In the simplest case, which we might call "unimodal" angular distributions, the net orientation arises from a preference for a moderate range of angular motion of each principal axis about its average orientation. This is most likely to occur for very strong local orientation but could occur for moderate or even weak local orientation. The principal axes can then be thought of as approximate symmetry axes of the angular motion. If in addition one eigenvalue is large and positive (i.e., oriented preferentially along the space-fixed *z*-axis), then the principal axes and their eigenvalues also provide a rough idea of the preferred average orientation of the molecule. In one example of a unimodal distribution, all three axes might fluctuate about their average positions in uncorrelated fashion. Alternatively, the molecule might rock primarily about a particular principal axis, causing correlated fluctuations in orientation of the other two axes.

In the discussion below, we attempt to understand the strong orienters (and also the moderate orienters) in terms of simple unimodal models consistently based on two familiar concepts. First, each amide prefers to direct its hydrogen-bonding carbonyl, and to a lesser extent its −NH groups, "outward" from the bicelle where they find water and carboxyl groups. Theory shows that the strongest hydrogen bonds to water bridge a carbonyl and a cis −NH group (CO···water···HN), having $\Delta H \cong -9.7$ kcal/mol compared with −7.5 kcal/mol for single carbonyl−water bonds and −6.1 kcal/mol for single −NH− water bonds.[18] The most important factor is exposure of the carbonyl group to water because it can make two or three useful hydrogen bonds while −NH makes only one. Second, an amide prefers to simultaneously orient a methyl group "inward", inserting it into the fluorocarbon core of the bicelle and shielding it from water. Amide-dependent conflicts between these preferences necessarily arise, forcing compromise on the angular distributions. We will find good evidence for these factors and will be able to judge their relative importance semiquantitatively to some extent. These interpretations gain some credence from their consistency but should be viewed with caution. It is important to remember that many "multimodal" distributions consistent with the data could easily be concocted.

Especially for *N*,*N*-DMF, the large magnitude of the eigenvalues of the **S** matrix strongly suggests preferential partitioning to the interface. The argument involves division of the entire volume of solution into three parts: bicelle interior, bicelle−water interface, and bulk water. The relative sizes of CsPFO and the amides of interest are depicted in Figure 9. By analogy to the more extensively studied lipid bilayer/water interface,[34] the bicelle−water interface between the packed fluorocarbon chains of the bicelle core and bulk exterior water is presumably a region rich in carboxyl groups, Cs^+ counterions, and water itself. Assume the amide resides only in the interface and in bulk water and not in the bicelle itself. Each order parameter then factors as $S_{ij} = f_{int} S_{bicelle} S^{ij}_{local}$. Here f_{int} is the equilibrium fraction of the amide population that resides in the bicelle−water interfacial region, $S_{bicelle}$ is the orientational order parameter of the oblate, cylindrical bicelle itself, and S^{ij}_{local} is a "local order parameter" describing the average degree of orientation of the *ij* axis while the amide resides at the interface. The same model applies to each of the eigenvalues displayed in Figure 8 because these are the order parameters of the three principal axes.

For the smectic phase of CsPFO/water at 40 wt % and 23 °C, the experimental value of the bicelle order parameter in a 100 MHz magnet is already $S_{bicelle} = 0.9$,[35] and we do not expect much stronger orientation at 500 MHz. At 35 wt % CsPFO, the dimensions of the oblate bicelle disks were estimated by X-ray diffraction as 80 Å in diameter and 22 Å thick with the

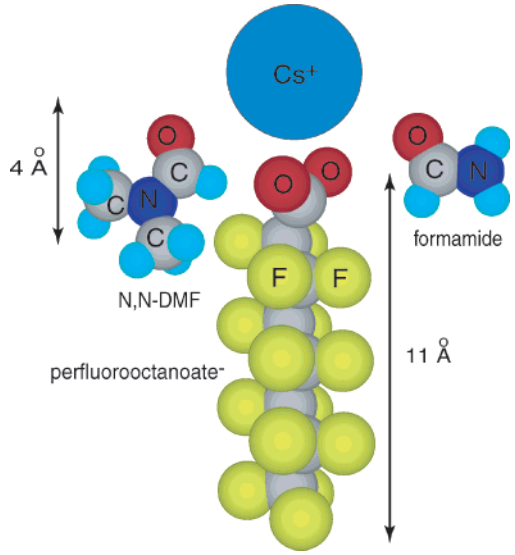

Figure 9. Scale model of CsPFO monomer with *N,N*-DMF and formamide. Geometries were optimized with MM2. Cs^+ atomic radius was taken as 1.7 Å.

bicelles occupying 0.186 of the total volume.[8] For a perfectly oriented, cylindrical bicelle of those dimensions, 64.5% of the bicelle surface is oriented horizontally and 35.5% vertically, which limits S^{ij}_{local} to the approximate range +0.468 to −0.234. Estimation of f_{int} requires the volume fraction of the interface, which requires an effective interfacial thickness. More precisely, the relevant thickness is the range of motion of the amide relative to the fluorocarbon chain in the direction normal to the bicelle−water interface over which the methyl group can make good contact with fluorocarbon and avoid water while the carbonyl group maintains good access to water. The scale model in Figure 9 suggests a distance of 3−4 Å, comparable to the vertical distance between the carboxyl oxygens and the second $-CF_2-$ group. We centered this thickness on the bicelle dimensions above and computed the fraction of the total volume due to bulk water, interface, and fluorocarbon core. Based on a 4 Å thickness, the result is 75.8% water, 10.6% interface, and 13.7% core, yielding $f_{\text{int}} = 0.122$ if the amide partitions without preference between the interface and the bulk water only. This would constrain all S_{ij} to lie in the range +0.0513 (perfect orientation normal to the bicelle surface) to −0.0256 (perfect orientation in the plane of the surface). An estimated thickness of 3 Å yields the range +0.0390 to −0.0195.

The two strong orienters have order parameters substantially larger than these estimates. With the signs chosen as in Figure 8, *trans-N*-methylformamide has $S_a = +0.093$ for its *a*-axis and $S_b = -0.054$ for its *b*-axis. *N,N*-DMF has $S_a = +0.148$ for its *a*-axis and $S_c = -0.084$ for its *c*-axis. These values are uncomfortably large unless we invoke some combination of strong local orientation within the interface and preferential partitioning to the interface. The opposite sign choice leads to even larger negative eigenvalues for both strong orienters. To turn the argument around, if there were no preferential partitioning in *N,N*-DMF, the value $S_c = -0.084$ would require an effective interfacial thickness of 14 Å, much larger than is reasonable. It appears that the concentration of amide at the interface must be higher than that in the bulk by a factor of 2 or more for *trans*-NMF and by a factor of 3 or more for *N,N*-DMF.

We have additional circumstantial evidence indicating strong attraction and preferential partitioning of *N,N*-DMF to the bicelle−water interface. The isotropic to nematic transition temperature is sensitive to *N,N*-DMF mole fraction at mole fractions above 0.0005, the concentration at which the spectrum of Figure 7 was obtained. For a 34 wt % CsPFO sample with DMF mole fraction of 0.004, the transition temperature is more than 5 °C lower than its value in the absence of amide.[16] This occurred only for *N,N*-DMF and not the other amides. For comparison, at a formamide mole fraction of 0.006, the transition temperature decreased by 1−2 °C or less. Clearly *N,N*-DMF interacts with the bicelle more strongly than the other amides.

B. Orientation Mechanism. What is the driving force underlying the attraction to the interface and strong orientation therein for three amides but not the others? For proteins in more weakly orienting lyotropic liquid crystals, protein *shape* provides a semiquantitative explanation of the detailed orientation tensor based on steric exclusion of certain orientations of the protein in the vicinity of the interface.[24] However, our amides have longest dimensions of only 4−5 Å (Figure 9), so molecular shape seems largely unimportant here. For comparison, if the bicelles are placed on a rectangular lattice that makes the volume fraction 19% and the bicelle−bicelle distance of closest approach the same in all directions, that distance is about 20 Å. In addition, the simple amides become more spherical as bulky methyl groups are added, yet they tend to orient somewhat more strongly. Also, shape alone would not explain the preferential partitioning of the strong orienters to the interface.

Electrostatic forces cannot explain the observed range of orientation strengths. The interaction of the interfacial electric field **E** with the molecular electric dipole moment μ_{el} can produce net orientation.[36] In the usual series expansion of the Boltzmann factor, $P(\Omega) = \exp(-E(\Omega)/(k_B T))$, where $E(\Omega)$ is the orientational energy, the term $-(\mu_{\text{el}}\cdot\mathbf{E})/(k_B T)$ makes no contribution to dipolar couplings because of its symmetry[2] but the term $^1/_2(\mu_{\text{el}}\cdot\mathbf{E})^2/(k_B T)^2$ does contribute to dipolar coupling. However, the variation in dipole moment among these amides is only 10% as judged by ab initio electronic structure calculations on the gas-phase molecules[29] and by mixed QM/MM simulations in water.[37] So the variation in the electric field contribution to orientation across molecules will be very small.

The solubility of substituted formamides in bulk water decreases as one, two, and three methyl groups are added,[38] and presumably alkyl groups are more soluble in fluorocarbon than in water. This suggests that amides with more methyl groups should partition more strongly to the interface, perhaps contributing to the moderately stronger orientation of *N*-methylacetamide and *cis-N*-methylformamide compared with formamide itself. However, the number of methyl groups alone cannot explain why acetamide and *cis-N*-methylacetamide orient comparably, why *cis-* and *trans-N*-methylformamide orient so differently, why *cis-N*-methylacetamide and *N,N*-dimethylformamide orient so differently, etc.

Clearly the *position* of the methyl groups is important. In all cases, strong orientation correlates with a methyl group lying trans to the carbonyl group. Whenever a hydrogen atom lies trans to carbonyl, the orientation strength is moderate or weak, regardless of the number or position of other methyl groups. This suggests that the strong orienters *trans-N*-methylformamide and *N,N*-dimethylformamide (and *N,N*-dimethylacetamide) insert the trans methyl group into the fluorocarbon core of the bicelles while simultaneously directing the polar carbonyl group "outward" toward the region rich in water and carboxyl groups with which it can hydrogen bond. Assuming the sign choices in Figure 8, the **S** tensors for the two strong orienters are consistent with this idea. The large absolute magnitudes of the principle values suggest a *unimodal orientational distribution* of the amide

within the interface, although other types of distribution are possible. In both molecules, S_b and S_c are similar in magnitude and about $-1/2$ of S_a. Accordingly, the trans methyl group axis (and thus the carbonyl axis) lies close to the *a*-axis and orients predominantly perpendicular to the bicelle surface ($S \cong +0.1$), while the *b*- and *c*-axes orient predominantly parallel to the bicelle surface ($S \cong -0.05$). The present case of very strong average orientation lends credence to this simple interpretation of the **S** tensor. The same picture places the electric dipole moment of the amides, which lies close to the N···O axis, in a favorable orientation relative to the interfacial electric field.

1. Strong Orienters. Assuming a unimodal distribution, *trans*-NMF orients its single methyl group perpendicular to the bicelle−water interface on average because the methyl axis coincides with the *a*-axis. This minimizes exposure of the methyl group to the watery interface while maintaining exposure of both the carbonyl group and the ND group to the hydrogen-bonding environment of the interface. Electronic structure theory applied to hydrogen bonding between a single water molecule and *cis*-*N*-methylacetamide found a highly favorable bridging hydrogen bond of structure CO···water···HN, with binding energy of 9.7 kcal/mol (B3LYP density functional).[18] This is substantially stronger than the nonbridging hydrogen bonds between water and carbonyl (7.5 kcal/mol) or between water and NH (6.1 kcal/mol). Thus *trans*-NMF can insert its methyl group into the fluorocarbon interior of the bicelle while simultaneously forming a strong bridging hydrogen bond to water in the interfacial region. The detailed eigenvalues indicate that the *b*-axis is most strongly oriented, but orientation within the interface is imperfect. That is, S_a is smaller than -2 times S_b by 14%, and S_c is smaller than S_b by 28%. One motional model that is quantitatively consistent with the ratio $S_a/S_c = -2.38 \pm 0.07$ invokes perfect orientation of the *b*-axis in the plane of the bicelle interface while the molecule rocks about the *b*-axis by some $\pm 30°$, sampling all rocking angles within that range uniformly. (Note that when averaged over azimuthal angles, such pure rotation about a single axis averages $P_2(\cos\theta)$ over a uniform distribution of θ, not an isotropic distribution, which would be weighted by $\sin\theta$). Formation of the bridging hydrogen bond CO···water···HN and insertion of the methyl group into the bicelle core can be well maintained throughout such motion. The motion need not be limited to pure rotation of the amide; it is more likely a combination of rotation of the amide and relative translation of local amide−fluorocarbon distances, that is, rocking can be coupled to corrugation of the interface. Of course, other angular averages could produce the same ratio S_a/S_c, but simple rotation of a limited range about the *b*-axis at least gives a sense of the strength of orientation.

In *N*,*N*-DMF, the carbonyl group can make two hydrogen bonds to water but the unusually strong bridging hydrogen bond is not available. It is not possible to bury both methyl groups in the fluorocarbon core at the same time. The order parameters (Table 6) show that the cis and trans methyl groups do not orient equivalently. In the unimodal interpretation, the average orientation of the trans methyl group axis tilts 21° away from the bicelle normal (*a*-axis) while the cis methyl axis tilts 86° away from the bicelle normal. *N*,*N*-DMF seemingly sacrifices the possibility of placing both methyl axes at 60° relative to the interfacial plane, which would place the carbonyl axis nearly *parallel* to the plane, in favor of placing one methyl axis nearly perpendicular to the plane. This allows better access of the carbonyl to interfacial water but orients the second methyl axis roughly parallel to the plane on average, partially exposing it to water. The eigenvalue ratios indicate that *N*,*N*-DMF is not rigidly oriented in the interface. The out-of-plane *c*-axis is most strongly oriented; S_a is smaller than -2 times S_c by 12%, and S_b is smaller than S_c by 24%. The ratio $S_a/S_b = -2.31 \pm 0.07$ is quantitatively consistent with perfect orientation of the *c*-axis in the plane of the bicelle interface while the molecule rocks about the *c*-axis by $\pm 28°$, sampling all rocking and azimuthal angles uniformly.

2. Moderate and Weak Orienters. Comparison of the moderate orienters *cis*-NMF and acetamide with the strong orienter *trans*-NMF is perhaps most appropriate because all three have similar sizes and one methyl group. If we assume the signs of Figure 8 are correct, then the moderate orienters would appear to follow the same general principles as the strong orienters. The pattern of eigenvalues is then similar to that of *trans*-NMF: large, positive in-plane S_a and in-plane S_b more negative than out-of-plane S_c. Neither *cis*-*N*-methylformamide nor acetamide can orient its methyl group perpendicular to the interfacial plane while directing the carbonyl group outward. In both cases, the preferred average orientation as judged by the **S** matrix seems to be a compromise between optimizing hydrogen bonding and partially burying methyl in the fluorocarbon core. This suggests that in *cis*-NMF it is more favorable to expose carbonyl to water than the ND group. Accordingly, carbonyl can make two or even three hydrogen bonds to water, while ND makes only one. According to electronic structure calculations, the first carbonyl−water bond is stronger than an ND−water bond by 1−2 kcal/mol.[18] Acetamide orients on average in a way that allows the highly favorable CO···water···HN bridge to form. The alternative choice of signs for *cis*-NMF would orient *both* the carbonyl and methyl axes roughly "up" or "down", in conflict with the ideas that seem to work so well for the strong orienters. For acetamide, the lower sign choice is problematic in much the same way.

The overall strength of orientation is 6−10 times weaker for the moderate orienters than for the strong orienters, as judged by S_{rms}. According to the relation $S_{ij} = f_{\mathrm{int}} S_{\mathrm{bicelle}} S^{ij}_{\mathrm{local}}$, weaker net orientation implies a smaller product $f_{\mathrm{int}} S^{ij}_{\mathrm{local}}$, but again it is difficult to separate the effect of partitioning from weaker local orientation of the amide within the interface. The data are quantitatively consistent with the following suggestion. The strong orienters are more concentrated in the interface than the bulk by a factor of 2−3 and orient quite rigidly while residing in the interface, as detailed above. The moderate orienters do not partition preferentially and have only about $1/3$ of the maximum possible local orientational order while residing in the interface.

Of course other combinations of preferential partitioning and local orientation strength can produce the same factor of 6−10. One could imagine an interfacial medium for which preferential partitioning of solute to the interface occurs without strong local orientation. However, for amides in CsPFO/water, we believe that these are closely related phenomena, even two sides of the same coin. The reason is the clear connection between methyl position and overall orientation strength. In the strong orienters, the quality of hydrogen-bonding opportunities alone would not drive partitioning to the interface; opportunities to hydrogen bond with water abound in the bulk. Evidently the ability to form good hydrogen bonds while simulatneously shielding methyl groups from water by inserting them into fluorocarbon drives both partitioning and orientation.

More quantitatively, we suggest that for the moderate orienters the "corrugation" of the mean-field potential vs orientation angle for the amide in the interface is comparable to $k_B T$, yielding local orientational order parameters about $1/3$

of the maximum possible. Yet the orientationally averaged mean field potential at the interface differs little from the bulk, so there is little preferential partitioning. For the strong orienters, the corrugation of the mean-field potential is larger, perhaps $(2-3)k_BT$, giving very strong local orientation. At the same time, the orientationally averaged mean-field potential at the interface is about $(1-2)k_BT$ lower than that in the bulk, leading to greater concentration of amide at the interface by a factor of 2 or more.

Among the two weak orienters, we have absolute signs for the **S** matrix of formamide only. Lacking hydrophobic groups, formamide is highly soluble in water. It could conceivably preferentially partition to the *bulk*, diminishing net orientation. Alternatively, we suggest that formamide is so small (largest internuclear distances below 4 Å) that it can probably fit comfortably in the interfacial region while simultaneously maintaining good hydrogen bonds to carbonyl and to both NH groups at essentially *any* orientation, as suggested in Figure 9.

For *trans*-NMA, the sign choice in Figure 8 is less clearly motivated than for the other amides. For a unimodal distribution, the signs as given would preferentially orient the acetyl methyl group vertically, allowing that methyl to insert into the fluorocarbon core while the carbonyl was exposed to water, much as in acetamide. The alternative choice has eigenvalues $S_a = -0.0039$, $S_b = +0.0067$, and $S_c = -0.0028$, and $S_{rms} = 0.0047$; note that in this one case these eigenvalues differ substantially in magnitude from the eigenvalues resulting from the sign choice of Figure 8. For a unimodal distribution, this alternative choice would orient the long axis of the molecule roughly parallel to the interfacial plane. If *trans*-NMA behaves as a composite of *cis*-NMF and acetamide, a bimodal distribution might occur and lead to the alternative sign set. It seems unwise to interpret such weak orientation in terms of a unimodal angular distribution, and the ratio of eigenvalues does not suggest a clear mechanism.

Finally, the earlier work on the much larger molecule alanine dipeptide in the same CsPFO/water medium showed that a particular conformation called P_{II} is dominant.[17,21,22] P_{II} orients about eight times more weakly than the two strongly orienting amides; it is comparable to the "moderate orienters" *N*-methylacetamide and *cis*-*N*-methylformamide. Accordingly, all relevant conformers of alanine dipeptide have NH, not $N-CH_3$, in the position trans to the amide carbonyls. Extension of the ideas presented here led to the suggestion that P_{II} would prefer to expose its two CO···HN water-binding "pockets" to hydrogen-bonding environs while dipping one or both methyl groups in the fluorocarbon core of the bicelle. This idea indeed gives a good semiquantitative understanding of the **S** matrix extracted from the data.

V. Conclusion

The quantitative differences in orientation strengths among the seven amides studied are striking. The physically appealing interpretation of strong orientation arising only when the amide can immerse its carbonyl group in interfacial water while simultaneously inserting a trans methyl group in the fluorocarbon core of the bicelle is quantitatively consistent with the derived **S** matrices for a particular choice of signs. However, we determine **S** only within a factor of ± 1. If more sophisticated two-dimensional NMR experiments could determine the absolute sign of even one dipolar coupling, all sign ambiguities would vanish. We have argued that at least for the strongest orienter *N*,*N*-DMF, the **S** tensor requires a combination of preferential concentration partitioning at the interface and very strong orientation while the amide resides there. Field gradient measurements of amide diffusion in liquid crystalline CsPFO/water might yield the degree of concentration partitioning independently, leading to a more quantitative picture of partitioning vs local orientation. Finally, our measurements provide an experimental benchmark against which to compare molecular dynamics simulations on these systems. Such simulations, even with the fluorocarbon cores kept rigid, would undoubtedly reveal many more fascinating details of the motion of these simple amides at the bicelle−water interface.

Acknowledgment. We thank the National Science Foundation for support of this work under Grant CHE-0077517. Prof. Ed Samulski and Dr. Chi-Duen Poon of University of North Carolina-Chapel Hill helped to conceive and launch this project while J.C.W. was on sabbatical leave there, and we thank them for their insights and hospitality. Dr. Charles Fry in the Chemical Instrumentation Center of the UW-Madison Chemistry Department made important technical contributions as well.

Supporting Information Available: Oriented ^1H spectrum of unlabeled *N*,*N*-DMF in 35 wt % CsPFO/D_2O at 21 °C, best-fit parameters from dipolar-coupled NMR spectrum of *N*,*N*-DMF in 35 wt % CsPFO/D_2O at 21 °C, and detailed coordinates of the gas-phase geometries of each molecule. This material is available free of charge via the Internet at http://pubs.acs.org.

References and Notes

(1) Saupe, A.; Englert, G. *Phys. Rev. Lett.* **1963**, *11*, 462.
(2) *Nuclear Magnetic Resonance of Liquid Crystals*; Emsley, J. W., Ed.; D. Reidel: Dordrecht, Netherlands, 1985.
(3) Emsley, J. N.; Lindon, J. C. *NMR Spectroscopy Using Liquid Crystal Solvents*; Pergamon Press: Oxford, U.K., 1975.
(4) Photinos, D. J.; Poliks, B. J.; Samulski, E. T.; Terzis, A. F.; Toriumi, H. *Mol. Phys.* **1991**, *72*, 333.
(5) Samulski, E. T.; Berendsen, J. C. *J. Chem. Phys.* **1972**, *56*, 3920.
(6) Diehl, P. Structure of Rigid Molecules Dissolved in Liquid Crystalline Solvents. In *Encyclopedia of Nuclear Magnetic Resonance*; Grant, D. M., Harris, R. K., Ed.; John Wiley and Sons, Ltd.: New York, 1996; Vol. 5, p 4591.
(7) Boden, N.; Clements, J.; Jolley, K. W.; Parker, D.; Smith, M. H. *J. Chem. Phys.* **1990**, *93*, 9096.
(8) Holmes, M. C.; Reynolds, D. J.; Boden, N. *J. Phys. Chem.* **1987**, *91*, 5257.
(9) Ottiger, M.; Bax, A. *J. Biomol. NMR* **1999**, *13*, 187.
(10) Koenig, B. W.; Hu, J. S.; Ottiger, M.; Bose, S.; Hendler, R. W.; Bax, A. *J. Am. Chem. Soc.* **1999**, *121*, 1385.
(11) Ottiger, M.; Bax, A. *J. Biomol. NMR* **1998**, *12*, 361.
(12) Ramirez, B. E.; Bax, A. *J. Am. Chem. Soc.* **1998**, *120*, 9106.
(13) Bax, A.; Tjandra, N.; Ottiger, M.; Marquardt, J.; Cornilescu, G.; Hu, J. S. *Biophys. J.* **1998**, *74*, A137.
(14) Losonczi, J. A.; Prestegard, J. H. *J. Biomol. NMR* **1998**, *12*, 447.
(15) Prestegard, J. H. *Abstr. Pap. Am. Chem. Soc.* **1997**, *214*, 202.
(16) Boden, N.; Corne, S. A.; Jolley, K. W. *J. Phys. Chem.* **1987**, *91*, 4092.
(17) Poon, C.-D.; Samulski, E. T.; Weise, C. F.; Weisshaar, J. C. *J. Am. Chem. Soc.* **2000**, *122*, 5642.
(18) Han, W. G.; Suhai, S. *J. Phys. Chem.* **1996**, *100*, 3942.
(19) Vaara, J.; Kaski, J.; Jokisaari, J.; Diehl, P. *J. Phys. Chem. A* **1997**, *101*, 5069.
(20) Sykora, S.; Vogt, J.; Bosiger, H.; Diehl, P. *J. Magn. Reson.* **1979**, *36*, 53.
(21) Weise, C.; Weisshaar, J. C. *J. Phys. Chem. A*, submitted for publication, 2002.
(22) Weise, C. Structure and Orientation of Alanine Dipeptide and of Small Amides in a Lyotropic Liquid Crystal. Ph.D. Thesis, University Wisconsin-Madison, Madison, WI, 2002.
(23) Gochin, M.; Pines, A.; Rosen, M. E.; Rucker, S. P.; Schmidt, C. *Mol. Phys.* **1990**, *69*, 671.
(24) Zweckstetter, M.; Bax, A. *J. Am. Chem. Soc.* **2000**, *122*, 3791.
(25) Keeler, A. J. S. a. J. *Prog. Nucl. Magn. Reson. Spectrosc.* **1987**, *19*, 47.
(26) Marat, K. *Program XSIM*, University of Manitoba: Winnipeg, MB, Canada, 1998.
(27) Chalmet, S.; Ruiz-López, M. F. *J. Chem. Phys.* **1999**, *111*, 1117.

(28) Frisch, M. J.; Trucks, G. W.; Schlegel, H. B.; Scuseria, G. E.; Robb, M. A.; Cheeseman, J. R.; Zakrzewski, V. G.; Montgomery, J. A., Jr.; Stratmann, R. E.; Burant, J. C.; Dapprich, S.; Millam, J. M.; Daniels, A. D.; Kudin, K. N.; Strain, M. C.; Farkas, O.; Tomasi, J.; Barone, V.; Cossi, M.; Cammi, R.; Mennucci, B.; Pomelli, C.; Adamo, C.; Clifford, S.; Ochterski, J.; Petersson, G. A.; Ayala, P. Y.; Cui, Q.; Morokuma, K.; Malick, D. K.; Rabuck, A. D.; Raghavachari, K.; Foresman, J. B.; Cioslowski, J.; Ortiz, J. V.; Stefanov, B. B.; Liu, G.; Liashenko, A.; Piskorz, P.; Komaromi, I.; Gomperts, R.; Martin, R. L.; Fox, D. J.; Keith, T.; Al-Laham, M. A.; Peng, C. Y.; Nanayakkara, A.; Gonzalez, C.; Challacombe, M.; Gill, P. M. W.; Johnson, B. G.; Chen, W.; Wong, M. W.; Andres, J. L.; Head-Gordon, M.; Replogle, E. S.; Pople, J. A. *Gaussian 98*, revision A.1; Gaussian, Inc.: Pittsburgh, PA, 1998.

(29) Wiberg, K.; Rush, D. J. *J. Org. Chem.* **2002**, *67*, 826.

(30) Reeves, L. W.; Riveros, J. M.: Spragg, R. A.; Vanin, J. A. *Mol. Phys.* **1973**, *25*, 9.

(31) Kamei, H. *Bull. Chem. Soc. Jpn.* **1968**, *41*, 2269.

(32) Khetrapal, C. L.; Kunwar, A. C.; Ramaprasad, S. *Mol. Cryst. Liq. Cryst.* **1976**, *34*, 123.

(33) Bourn, A. J. R.; Randall, E. W. *J. Mol. Spectrosc.* **1964**, *13*, 29.

(34) White, S. H.; Wiener, M. C. The liquid-crystallographic structure of fluid lipid bilayer membranes. In *Biological membranes: a molecular perspective from computation and experiment*; Merz, K. M., Jr., Roux, B., Eds.; Birkhauser: Boston, MA, 1996.

(35) Johannesson, H.; Furo, I.; Halle, B. *Phys. Rev. E* **1996**, *53*, 4904.

(36) Hiemenz, P. C.; Rajagopalan, R. *Principles of Colloid and Surface Chemistry*, 3rd ed.; Marcel Dekker Inc.: New York, 1997.

(37) Gao, J.; Pavelites, J. J.; Habibollazadeh, D. *J. Phys. Chem.* **1996**, *100*, 2689.

(38) Sangster, J. *J. Phys. Chem. Ref. Data* **1989**, *18*, 1111.